mobile wireless applications where less demanding than fully adaptive beam-formed far-field radiation-pattern responses are required.

## REFERENCES


[1] M. I. Skolnik and D. D. King, "Self-phasing array antennas," *IEEE Trans. Antennas Propagat.*, vol. AP-12, pp. 142–149, Mar. 1964.
[2] L. C. Van Atta, "Electromagnetic reflector," U.S. Patent 2 908 002, Oct. 1959.
[3] C. Y. Pon, "Retrodirective array using the heterodyne technique," *IEEE Trans. Antennas Propagat.*, vol. AP-12, pp. 176–180, Dec. 1964.
[4] P. V. Brennan, "An experimental and theoretical study of self-phased arrays in mobile satellite communications," *IEEE Trans. Antennas Propagat.*, vol. 37, pp. 1370–1376, Nov. 1989.
[5] T. Murata and M. Fujita, "A self-steering planar array antenna for satellite broadcast reception," *IEEE Trans. Broadcast.*, vol. 40, pp. 1–6, Mar. 1994.
[6] J. D. Kraus, *Antennas*, 2nd ed. New York: McGraw-Hill, 1988.
[7] R. C. Hansen, *Phased Array Antennas*. New York: Wiley, 1998.
[8] S. L. Karode and V. F. Fusco, "Phase conjugate circuit and retroreceive antenna," British Patent 9 904 179.0, Feb. 1998.
[9] M. J. Withers, D. E. N. Davies, A. H. Wright, and R. H. Apperley, "Self-focusing receiving array," *Proc. Inst. Elect. Eng.*, vol. 112, pp. 1683–1688, 1965.
[10] S. Gupta and V. F. Fusco, "Automatic beam steered active antenna receiver," in *Proc. IEEE MTT-S Int. Microwave Symp. Dig.*, 1997, pp. 599–602.
[11] J. R. James, G. D. Evans, and A. Fray, "Beam scanning microstrip arrays using diodes," *Proc. Inst. Elect. Eng.*, pt. H, vol. 140, pp. 43–51, 1993.
[12] S. C. Swales, M. A. Beach, D. J. Edwards, and J. P. McGeehan, "The performance enhancement of multibeam adaptive base station antennas for cellular land mobile radio systems," *IEEE Trans. Veh. Technol.*, vol. 39, pp. 56–67, Feb. 1990.


# Measurement of Two-Tone Transfer Characteristics of High-Power Amplifiers

Youngoo Yang, Jeahyok Yi, Joongjin Nam, Bumman Kim, and Myungkyu Park

***Abstract*—In this paper, we present an accurate measurement method for acquiring the two-tone transfer characteristics of high-power amplifiers. The measurement setup and sequence are described. The measured amplitude and phase data of the two-tone fundamental, third-order intermodulation, and fifth-order intermodulation components versus input power level are also presented. The measured two-tone transfer characteristics are very useful for the design of a predistortion linearizer or for nonlinear model extraction for high-power amplifiers.**

***Index Terms*—AM–AM, AM–PM, high-power amplifier, memory effect, two-tone transfer characteristics.**

## I. INTRODUCTION

The behavioral or mathematical model of power amplifiers has been studied extensively. A small class-A power amplifier has normally been treated with the assumption that is a memoryless (Taylor series representation of AM–AM characteristics only) or quasi-memoryless (complex representation of Taylor series with both AM–AM and AM–PM characteristics) system [1]–[5]. However, the characterization of a very high-power amplifier with an output power of over a few hundred watts has not been reported yet. Multistage high-power, class-AB or class-B amplifiers generally have a large memory effect and strong nonlinearity. The single-tone transfer characteristics based on AM–AM and AM–PM conversion cannot properly express the nonlinearity of these high-power amplifiers. Bosch *et al.* reported on a case where a predistortion linearized amplifier with improved AM–AM and AM–PM characteristics did not provide any enhancement on the two-tone intermodulation (IM) nonlinearity [6]. Therefore, more accurate two-tone characterization with phase information should be developed.

A method for measuring the relative phase of third-order intermodulation (IM3) compared to the phase of input signal has been presented by Suematsu *et al.* [7]. His method is based on the assumption that, in the weakly nonlinear region, the relative phase of IM3 is equal to the relative phase of fundamental. To verify the measured relative phase of IM3, they employed Volterra-series analysis based on the measured single-tone characteristics (AM–AM and AM–PM). Unfortunately, his assumption is not valid for most high RF power amplifiers. For a wide range of gate biases in GaAs MESFETs, the third-order Volterra-series coefficient of transcunductance (gm3) has reversed polarity to gm [8]–[10]. This means that the relative phase of IM3 may be $180^\circ$ out of phase to the fundamental output. Moreover, he overlooked the internal device capacitance effect on the phase variation. At a high frequency, these capacitances may change the phases of fundamental and IM3. These phase variations can be easily verified through a harmonic-balance simulation with a large-signal model of MESFETs.

In this paper, we present a new accurate measurement technique for determining the two-tone transfer characteristics of high-power amplifiers. The relative phases of the harmonic terms of a very low-frequency amplifier are $0^\circ$ or $180^\circ$. A small power GaAs MESFET amplifier at 750 kHz is used for the reference IM generator. For the measurement, the amplifier output is down-converted to the IF frequency and the relative phase is measured by comparing with the reference signal. A 500-W class-AB multistage power amplifier is used for the measurement. The measurement setup and sequence are described and the measured results are shown.

## II. EXPERIMENT

### A. Main Amplifier Under Test

A four-stage amplifier is built for Korea's wireless local loop (WLL) band of 2.37–2.4 GHz. Its final stage is built using four balanced 130-W amplifiers with Motorola's RF LDMOSFET MRF21120. It is a push–pull type with class-AB operation. The other three stages are arranged to drive the final stage amplifier. The peak output power at the 1-dB gain compression point is about 500 W and the overall gain is 44.5 dB. The operational average output power is 50 W with WCDMA signal input, which has a chip rate of 8.192 Mc/s. Fig. 1 depicts a line-up diagram of the main amplifier used for testing.

### B. Measurement Setup

The measurement setup is shown in Fig. 2. This setup requires many measurement instruments: a two-tone signal generator, a vector network analyzer, a two-input power meter, and two spectrum analyzers. The reference IM generator is a small power MESFET of Hewlett-Packard's ATF21186 and is operated at a very low center frequency of 750 kHz. In the low frequency, the memory effect of the device

Manuscript received Novmeber 2, 1999.

Y. Yang, J. Yi, J. Nam, and B. Kim are with the Department of Electronic and Electrical Engineering and the Microwave Application Research Center, Pohang University of Science and Technology, Namku Pohang 790-784, Korea (e-mail: alice@postech.ac.kr).

M. Park is with LG Information and Communication, Kumi, Kyungbuk, Korea.

Publisher Item Identifier S 0018-9480(01)01698-2.

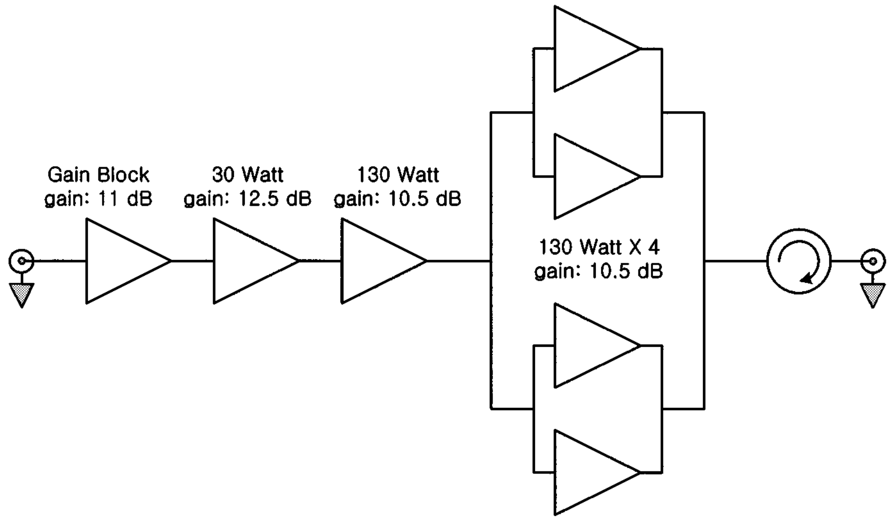


Fig. 1. Class-AB high-power amplifier module for test.

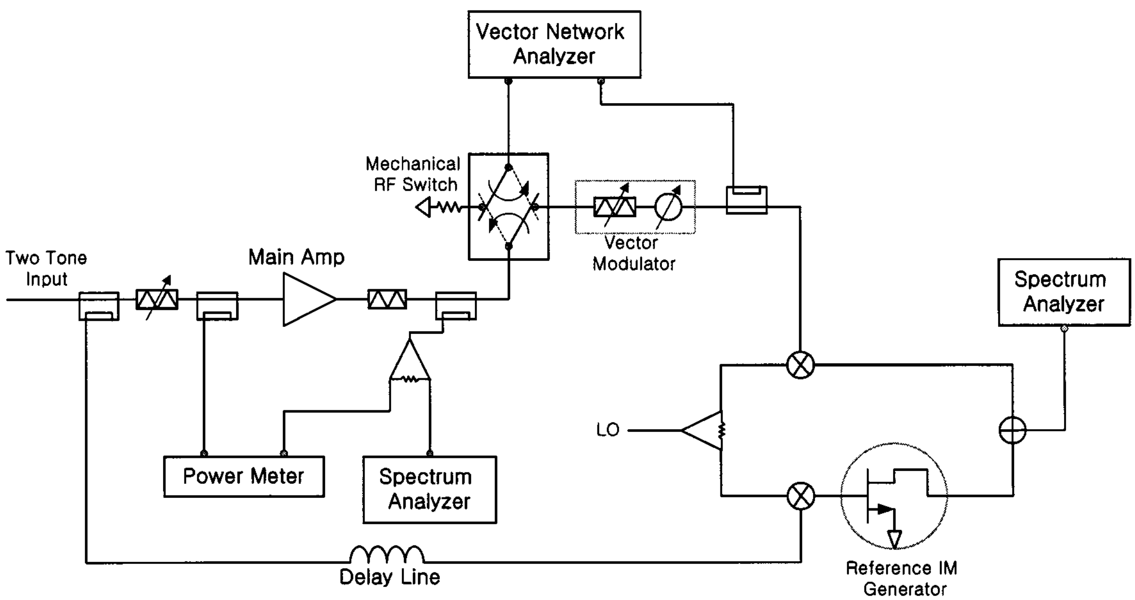


Fig. 2. Measurement setup for two-tone transfer characteristics.

can be ignored because its nonlinear capacitances are nearly open circuited and the propagation delay is negligible. Hence, the device has no AM–PM characteristics and its fundamental, IM3, and fifth-order intermodulation (IM5) show no phase variations with the input power level. This characteristic is verified by the two-tone harmonic-balance simulation using the large-signal model of the device. Fig. 3 shows the results of this simulation. The phases of fundamental, IM3, and IM5 are constant throughout the input power level up to the 1-dB gain compression point. Fundamental and IM5 have an equal phase and IM3 is 180° out of phase because the third-order Volterra-series coefficient (gm3) has a negative sign.

The two-tone input signal, which has a tone spacing of 100 kHz, is tapped to the reference path. The main path signal passes through the step attenuator for input power level control and is then coupled to power meter A for monitoring input power. The main amplifier output signal is attenuated and coupled to power meter B for monitoring output

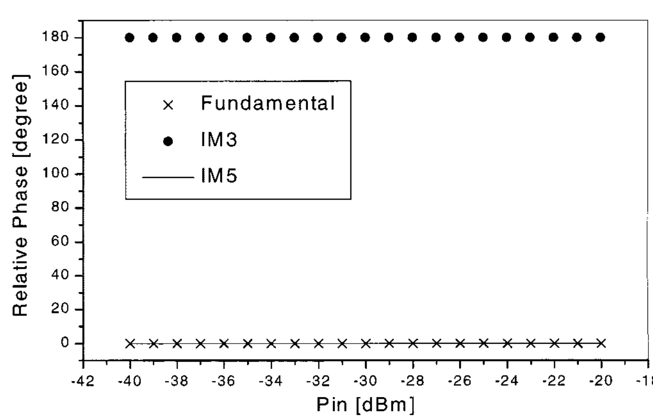


Fig. 3. Simulated relative phases of fundamental, IM3, and IM5 of reference IM generator as two-tone input power level at a center frequency of 750 kHz.

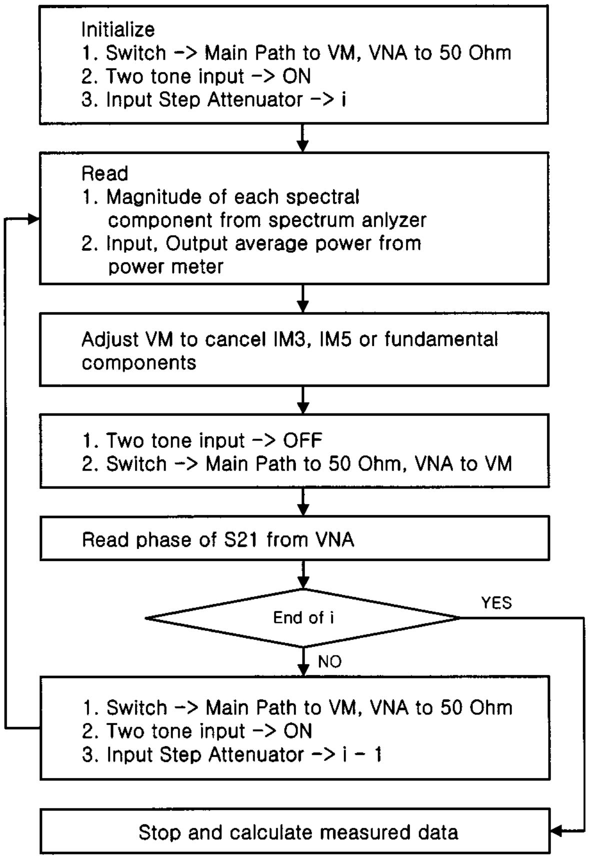


Fig. 4. Measurement sequence flowchart.

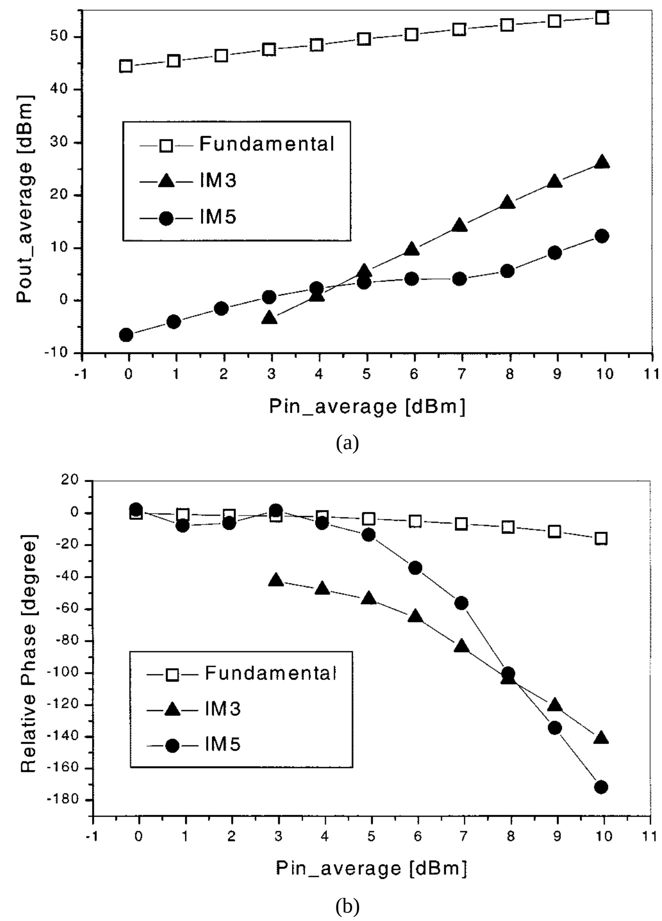


Fig. 5. Measured results of two-tone transfer characteristics. (a) Amplitude. (b) Phase.

power and to the spectrum analyzer for the relative power measurement of IM3 and IM5. The vector modulator, which consists of a variable attenuator and variable phase shifter, is used to adjust the amplitude and phase of the fundamental, IM3, or IM5 component of the output signal in order to cancel the corresponding reference signal component at the adder.

Finally, the output signal and reference signal are down-converted to a very low frequency (around 750 kHz) by the proper local oscillator (LO) signal. The down-converted reference signal is amplified by the reference IM generator and the reference IM terms are generated. The output and reference signals are canceled using an analog adder circuit. This low-frequency part may well be shielded to block out environmental noise. The vector network analyzer measures the required phase variation of the vector modulator for the cancellation by reading the phase of $S_{21}$. The mechanical RF switch connects and disconnects the loop without breaking calibration.

### C. Measurement Sequence

The complete flow of the measurement sequence is shown in Fig. 4. For the initialization, vector network analyzer port 1 is connected to 50-$\Omega$ load and the main path is connected to a vector modulator by a mechanical RF switch, the two-tone input is ON, and the input step attenuator is set to an appropriate starting power level. The input and output powers are read from the power meter and the relative amplitudes of fundamental, IM3, and IM5 are acquired from the spectrum analyzer. The vector modulator is then adjusted to cancel the fundamental, IM3, or IM5 components. After adjustment has been done, the two-tone input is OFF at the signal generator and the RF switch changes the connection of vector-network-analyzer port 1 to vector modulator and the main path to 50-$\Omega$ load in order to measure the relative phase variation of the vector modulator. After reading the phase of $S_{21}$ from the vector network analyzer, the RF switch connects the main path to the vector modulator, the two-tone input is ON, and input step attenuator is set to increase the input power level.

This sequence is repeated for the measurement of fundamental, IM3, and IM5 phases until the output power of the main amplifier is saturated. The measured data provide the relative phase variations of the fundamental, IM3, and IM5 components of the main amplifier. The reference IM3 phase offset of 180° is deembeded from the measured relative phase of IM3.

## III. Results

More than 30-dB cancellation has been achieved for the fundamental components. A 30-dB cancellation gives about a $\pm 1.8°$ phase error bound if the amplitudes of two branches are perfectly matched. However, for IM3 and IM5, the cancellation cannot reach as high as 30 dB at a low-input power level due to the noise floor level of the spectrum analyzer. In the case of 10-dB cancellation, for example, the relative phase error bound is increased to $\pm 10°$, if the amplitudes of the main path and reference path are perfectly matched. However, the relative phase error bound can be drastically reduced (to $\pm 1.5°$) when the amplitude mismatch between the two branches is 0.84 dB and a 10-dB cancellation is maintained. To obtain highly accurate measurement data of the relative phases of fundamental, IM3, and IM5 components, a proper amplitude mismatch condition should be applied.

Fig. 5 shows the measured amplitude and phase characteristics of the high-power amplifier under test. The two-tone average output powers of fundamental, IM3, and IM5 are plotted in Fig. 5(a). The measured relative phases are plotted in Fig. 5(b). The first measurement point of fundamental is set to zero phase and the others are calculated to have relative values. The measured phases of IM3 and IM5 vary rapidly as the power level approaches saturation.

## IV. Conclusion

To adequately consider the memory effect for high-power amplifiers, we have presented a new accurate method for measuring two-tone transfer characteristics. We measured the characteristics of a multistage high-power amplifier with a 500-W power output and 44.5-dB gain. We have used a trustworthy reference IM generator at a very low frequency. The two-tone harmonic balance simulation shows the accuracy of the relative phase of the reference IM generator. The complete measurement setup and sequence have been described.

We measured the relative phases of fundamental, IM3, and IM5. The measured data of IM3 and IM5 are very smooth and continuous, and vary rapidly as the power level approaches the output power saturation. The measured two-tone transfer characteristics are very useful for the design of predistortion linearizer or nonlinear model extraction for high-power amplifiers.

## References

[1] K. G. Gard, H. M. Gutierrez, and M. B. Steer, "Characterization of spectral regrowth in microwave amplifiers based on the nonlinear transformation of a complex Gaussian process," *IEEE Trans. Microwave Theory Tech.*, vol. 47, pp. 1059–1069, July 1999.

[2] Q. Wu, H. Xiao, and F. Li, "Linear RF power amplifier design for CDMA signals: A spectrum analysis approach," *Microwave J.*, pp. 22–40, Dec. 1998.

[3] C. J. Clark, G. Chrisikos, M. S. Muha, A. A. Moulthrop, and C. P. Silva, "Time-domain envelope measurement technique with application to wide-band power amplifier modeling," *IEEE Trans. Microwave Theory Tech.*, vol. 46, pp. 2531–2540, Dec. 1998.

[4] A. Leke and J. S. Kenny, "Behavioral modeling of narrowband microwave power amplifiers with applications in simulating spectral regrowth," in *IEEE MTT-S Microwave Symp. Dig.*, 1996, pp. 1385–1388.

[5] S. Chen, W. Panton, and R. Gilmore, "Effects of nonlinear distortion on CDMA communication systems," *IEEE Trans. Microwave Theory Tech.*, vol. 44, pp. 2743–2750, Dec. 1996.

[6] W. Bosch and G. Gatti, "Measurement and simulation of memory effects in predistortion linearizers," *IEEE Trans. Microwave Theory Tech.*, vol. 37, pp. 1885–1890, Dec. 1989.

[7] N. Suematsu, Y. Iyama, and O. Ishida, "Transfer characteristics of IM3 relative phase for a GaAs FET amplifier," *IEEE Trans. Microwave Theory Tech.*, vol. 45, pp. 2509–2514, Dec. 1997.

[8] S. A. Maas and D. Neilson, "Modeling MESFET's for intermodulation analysis of mixers and amplifiers," *IEEE Trans. Microwave Theory Tech.*, vol. 38, pp. 1964–1971, Dec. 1990.

[9] J. C. Pedro and J. Perez, "Accurate simulation of GaAs MESFET's intermodulation distortion using a new drain-source current model," *IEEE Trans. Microwave Theory Tech.*, vol. 42, pp. 25–33, Dec. 1997.

[10] T. M. Roh, Y. Kim, Y. Suh, and B. Kim, "A new simple extraction method for higher order components of channel current in GaAs MESFET," in *27th European Microwave Conf. Dig.*, Jerusalem, Israel, Sept. 1997, pp. 415–421.

# Integration Equation Analysis on Resonant Frequencies and Quality Factors of Rectangular Dielectric Resonators

Shyh-Yeong Ke and Yuan-Tung Cheng

***Abstract*—In this paper, the resonance problem of rectangular dielectric resonators (DRs) is analyzed by using the spectral dyadic Green's function and volume integral-equation formulation. The rectangular dielectric body is replaced by a set of entire-domain polarized volume current basis, and Galerkin's moment method is used to solve the resonant frequency and quality factor of the rectangular DR. The effects of electrical and geometrical parameters on the resonance of the $TE_{111}$ mode of isolated DRs are also presented. Additionally, the case of a rectangular DR with a ground plane is also discussed. Results are found to be in good agreement with the published experimental data.**

***Index Terms*—Dielectric resonators, method of moments.**

## I. Introduction

Dielectric resonators (DRs) are extensively used for microwave circuit components such as filters and antennas [1], [2]. Recently, open rectangular DRs for use as radiation elements have received increasing attention due to their simplified mechanism and easy integration with microwave integrated circuits (MICs). Besides, the microwave components made of high-permittivity dielectric materials have the advantages of small size and temperature stability. In the DR filter or DR antenna design, the quality factor is a very important consideration since it accounts for the loss (dielectric and radiation losses) of a DR. Furthermore, accurate prediction of the DR's resonant frequency is of interest in the design of a narrow-band component. A number of studies for rigorously evaluating the resonant frequencies and quality factors of cylindrical or rectangular box-like DRs have been reported. The surface integral formulation [3], the least-square method [4], the mode-matching method [5], and the finite-difference time-domain method [6] have been successfully used to investigate the resonance problems of cylindrical DR structures. However, the exact numerical method for analyzing electromagnetic problems of a three-dimensional structure often takes much CPU time. This motivates this present study of using an accurate and efficient numerical method to analyze the resonance problems of open rectangular DR structures.

In this paper, the resonant frequencies and radiation $Q$ factors of $TE_{111}$ modes of open rectangular DRs are investigated by using a volume integral-equation solution. The spectral dyadic Green's functions and electric-field integral equations are derived and described in the Section II. A set of entire-domain volume current basis is presented for efficiently calculating the complex resonant frequencies of rectangular DRs. In Section III, numerical results are presented and discussed. Finally, conclusions are presented in Section IV.

## II. Theory

### *A. Spectral Dyadic Green's Function and Integral-Equation Formulation*

Fig. 1 shows the geometry of the rectangular DR under consideration. The rectangular DR is with a dimension of $2W \times 2L \times 2h$ and a

Manuscript received November 16, 1999. This work was supported by the National Science Council, R.O.C., under Grant NSC88-2213-E145-006.

The authors are with the Department of Electrical Engineering, Chinese Military Academy, Kaohsiung, Taiwan 830, R.O.C. (e-mail: syke@cc.cma.edu.tw).

Publisher Item Identifier S 0018-9480(01)01699-4.